LA-UR -77-1754

TITLE: HEAT TRANSFER IN THE LITHIUM-COOLED BLANKET OF A PULSED FUSION REACTOR

AUTHOR(S): G. E. Cort and R. A. Krakowski

SUBMITTED TO: 6th International Heat Transfer Conference, Toronto, Ontario, Canada, August 7-11, 1978

los alamos
scientific laboratory
of the University of California
LOS ALAMOS, NEW MEXICO 87545

An Affirmative Action/Equal Opportunity Employer

MASTER

Form No. 836
St. No. 2629
1/75

UNITED STATES
ENERGY RESEARCH AND
DEVELOPMENT ADMINISTRATION
CONTRACT W-7405-ENG. 36

HEAT TRANSFER IN THE LITHIUM-COOLED BLANKET OF A PULSED FUSION REACTOR

G. E. Cort

R. A. Krakowski

Los Alamos Scientific Laboratory, University of California,
Los Alamos, New Mexico 87545 U. S. A.

ABSTRACT

The transient temperature distribution in the lithium-cooled blanket of a pulsed fusion reactor has been calculated using a finite-element heat-conduction computer program. An auxiliary program was used to predict the coolant transient velocity in a network of parallel and series flow passages with constant driving pressure and varying magnetic field. The coolant velocity was calculated by a Runge-Kutta numerical integration of the conservation equations.

The lithium coolant was part of the finite-element heat-conduction mesh with the velocity terms included in the total matrix. The matrix was solved implicitly at each time step for the nodal point temperatures. Slug flow was assumed in the coolant passages and the Boussinesq analogy was used to calculate turbulent heat transfer when the magnetic field was not present.

NOMENCLATURE

B = magnetic field, Tesla
k = Boltzmann constant
n = ion density
R = hydraulic radius of flow channels
Re = Reynolds number, uR/ν
T = temperature
u = velocity parallel to centerline

Greek Letters

β = ratio of plasma kinetic pressure to confining magnetic pressure = $2nkT/(B^2/2\mu_o)$
ΔP = total driving pressure for lithium flow
Λ = eddy thermal conductivity
$\mu_o = 4\pi \times 10^{-7}$ H/m
ξ = eddy dynamic viscosity
ν = kinematic viscosity

INTRODUCTION

Assuming that there will be significant advances in the physics of plasma confinement, the potential for controlled thermonuclear fusion for economic power production is being assessed. As part of the overall effort, conceptual but comprehensive engineering design studies have been made of a number of plasma confinement schemes (1-4). The magnetically confined systems that have been subjected to engineering evaluation can be classified as steady state (1), quasi-steady state (2), and pulsed (3). The mathematical modeling of neutronic/heat-transfer/structural aspects of the thermal-hydraulic, tritium-breeding blanket that surrounds a reacting deuterium/tritium plasma [T + D → n(14.1 MeV) + ^{4}He(3.5 MeV)] represents an integral part (5,6) of the overall technological assessment (7) provided by these fusion reactor studies. Particular attention must be given to all heat-transfer aspects of pulsed fusion concepts. Although the results of heat-transfer/blanket design calculations presented herein pertain specifically to the toroidal Reference Theta-Pinch Reactor (RTPR) (4), these results are generally applicable, with some modification, to other pulsed magnetically-confined fusion power concepts. The blanket structure (or "first wall") that directly faces the hot (10 to 30 keV)[1] reacting plasma represents a particularly crucial heat-transfer/thermal-stress problem, which has been treated in detail elsewhere (8). This paper focuses primarily on the thermal/hydraulic response of the entire liquid-lithium-cooled blanket.

The RTPR will operate as a high-β stellerator (4) where the plasma is heated compressionally by a magnetic field that does not penetrate the plasma during the confinement time. The RTPR must operate in a pulsed mode with thermonuclear burn time of 0.1 to 0.4 s. Important parameters associated with the RTPR pulsed power cycle are shown schematically in Fig. 1. The physical relationship between the plasma, blanket, and magnetic coils is shown in Fig. 2. The pulsed fusion reactor is composed of a series of these ~ 2-m-long modules arranged end-to-end. It should be emphasized that the segmented blanket structure serves as a magnetic flux concentrator on the implosion-heating time scale (~1 μs), and is divided into regions that are small enough to minimize eddy current losses on the adiabatic compression time scale (~30 ms). The blanket is otherwise electrically and mechanically decoupled from the magnetic coils and associated electrical circuitry.

Each cylindrical module of the segmented blanket is divided into 100 azimuthal sectors shown in more detail in Fig. 3. Each segment represents an

[1] 1 keV ~ 12.5 (10)^6 K.

independent flow system. The segments are subdivided into cells or cans containing flowing lithium coolant, stagnant molten lead (neutron multiplier), Li-6/tritium breeding material, and iron or boron-carbide shielding (Fig. 3). Alumina (electrical) insulator coatings between each azimuthal sector are also included, and the structural material is 1-mm-thick Nb-1Zr alloy. Other methods of fabrication have been considered as alternatives, but only the design in Fig. 3 has been subjected to detailed neutronic (9,10) and thermal analyses. Each blanket segment is fabricated from a flat sheet that is rolled into two matching halves and tack-welded together to form integral flow passages. This type of construction is commonly used for heat-exchanger panels (11), and leakage of lithium coolant between the plates under the tack welds is not detrimental to blanket performance. Hexagonal 0.5-mm-thick Nb-1Zr cans of stagnant liquid lead or lithium are inserted in the spaces between the coolant passages within the tritium-breeding region of the blanket. In the outer gamma-shielding region uncanned logs of iron or boron-carbide are inserted. Figure 3 has been simplified to show only some typical blanket layers; seven coolant ducts are actually considered necessary.

TRANSIENT HEAT TRANSFER WITH PULSED FLOW

The burn cycle parameters depicted in Fig. 1 were used with one-dimensional (cylindrical) neutronic calculations to provide the time-space dependence of the neutron and gamma-ray power densities. Figure 4 is a one-dimensional representation of the neutronic/heat-transfer calculational model and Table I summarizes the key parameters used in the blanket heat-transfer calculations. Because of the pulsed magnetic fields, liquid-lithium coolant flow will also be time dependent during the plasma burn and quench stages, and the time resolution of the coolant flow, therefore, represents an essential feature of the blanket heat-transfer calculation.

Figure 5 gives the liquid-lithium flow circuit for the blanket configuration depicted in Fig. 3. Because of the large pressure drop created by the magnetic field during the burn, the lithium coolant flow virtually ceases during this period. The transient and steady-state flow rates are calculated for each coolant leg depicted in Fig. 5. The

TABLE I. Parameters used in Blanket Heat-Transfer Calculations

Initial Blanket Temperature	1100 K
Coolant Inlet Temperature	1100 K
Duty Cycle	5 s
Rise Time of Compression Field	0.03 s
Compression Field, Flat-top Time	0.4 s
Plasma Cooling Time	2.0 s
Implosion Heating Magnetic Field	0.88 Tesla
Maximum Compression Field	7 Tesla
Quench Field	4 Tesla
Total Neutron and Gamma Energy	87.6 MJ/m
Bremsstrahlung Energy	1.44 MJ/m
Plasma Internal Energy, End of Burn	5.96 MJ/m

one-dimensional momentum equations for each coolant leg, subject to the conditions of mass continuity and pressure balance, are used to describe the flow transient. The flow equations are derived for a slightly different geometry in Ref. (12) by use of the following simplifying assumptions: 1. incompressible fluid, 2. constant properties, 3. zero electric field, and 4. neglect of gravitational forces and localized geometry effects at the manifolds. Based on a lithium sound speed of 4.2 km/s, the characteristic travel time for a pressure wave to reach the end of the 2-m module is ~1% of the time for the fluid to come to rest. Therefore, the flow transient is "slow" with respect to the wave velocity and inertial terms dominate. The transient surge flows, pressure oscillations, and lithium compressibility, therefore, are neglected for purposes of determining heat transfer in the blanket.

The nondimensional momentum equations (12) for each coolant leg (Fig. 5) are solved numerically by a Runge-Kutta integration for a given magnetic-field waveform to give the flow velocity. The pressure differential, ΔP, across the lithium inlet-outlet measured at a reference point outside the magnetic field (Fig. 5) is held fixed. In this way the flow condition within the magnetic field is decoupled from the external piping and surge tanks. The pressure drop resulting from flow across the pulsed magnetic field lines is taken into account only for the inlet and exit legs; ideally, the Hartmann number is zero for the other coolant legs with flow parallel to the magnetic field.

An important objective of the blanket design is to minimize the lithium flow rate and pumping power. Two approximate limits have been established for the lithium flow. The lower limit corresponds to the case where the flow barely achieves steady state at the end of a 5-s cycle time for a given flow geometry and magnetic field. The upper limit is set by the flow above which no significant improvement in blanket temperatures occurs because the rate of heat transfer is limited by conduction out of the solid (or stagnant liquid) regions. Parametric studies showed that these limits cover a rather narrow range from 0.0035 m^3/s per segment at ΔP = 5.1 kPa to 0.0125 m^3/s per segment at 51 kPa. The corresponding ideal pumping power per meter of length varies from 0.9 kWe to 30 kWe at peak flow for the 100 segments in a module. The blanket will theoretically operate at any intermediate flow provided the tradeoffs in pumping power, temperatures, and temperature cycle are acceptable.

The flow velocities in the inlet leg are shown in Fig. 6 for a range of ΔP values and the magnetic field time history indicated. The high-flow case (ΔP = 51 kPa) was chosen as a reference case because it results in the minimum temperatures and thermal stress in the blanket. The flow velocities in the seven 2-m-long coolant legs within the blanket follow a similar time history to that given in Fig. 6, but differ in magnitude because of differences in flow area.

HEAT TRANSFER IN PULSED FLOW BLANKETS

The blanket geometry pictured in Fig. 3 was modeled as a series of concentric annular regions (Fig. 4). The two-dimensional (r,z) heat-transfer model included convective terms where appropriate, but by symmetry neglected heat conduction in the azimuthal direction. A general purpose finite-element heat-conduction program, AYER (13), was used. The program implicitly solves the transient two-dimensional equation of heat conduction, including effects of inplane anisotropic conductivity, three-dimensional velocity distribution, and interface thermal contact resistance.

The neutron and (neutron-induced) gamma heating varies across the blanket by more than an order of magnitude and contains sharp discontinuities at the coolant channels (10). During the thermonuclear burn, the first wall intercepts bremsstrahlung energy flux, Fig. 1. After the 0.4 s of thermonuclear burn, the plasma internal energy is removed by a radially outward heat flow through a neutral-gas layer to the first wall (12,14). An important feature is that this rate of heat transfer is nearly constant with time (12). The total energy deposited in the blanket from each of the three heating mechanisms (neutron/gamma, plasma bremsstrahlung, and plasma dump) is summarized in Table I.

The lithium coolant is included in the finite-element mesh with the time-dependent velocities in each leg specified. The velocity is taken to be uniform in each coolant leg (slug flow), with heat transfer from the wall occurring by molecular conduction only in the presence of magnetic fields or when the flow is laminar. When the magnetic field is zero and the flow is turbulent (Re > 2000), an eddy conductivity is used to enforce the laminar formulation (Boussinesq analogy) (15) on the wall heat flux.

The eddy thermal conductivity, Λ, was found by combining Rohsenow and Cohen's (16) expression for the turbulent Prandtl number with Spalding's (17) "law of the wall" for the eddy dynamic viscosity, ξ. Through the use of the Blausius (15) relation for the wall friction, a representative value for Λ was found that is based on the average velocity. Although ξ and Λ vary with position in the general case, solutions for the temperature gradients in pipe flow show (18) that Λ is relatively constant for liquid metals. The resistance to heat flow is not found in the laminar sublayer or in the buffer layers, as is the case with other fluids, but is more evenly distributed throughout the cross section. The determination of ξ from an inner law or "law of the wall" (17) may be questioned, since the outer layer, or "law of the wake" appears to be more applicable. The decision to use the "law of the wall" was arbitrary, and was influenced by factors of convenience and conservatism (predicting lower heat-transfer rates). A conservative value for Λ is desirable because the turbulent eddies will probably be damped by the magnetic field. The principal advantage in using the eddy conductivity instead of a Lyon-type relationship (19) for convective heat transfer is the saving in computional effort with the finite-element mesh.

Thermal contact resistance between the metal cans (Fig. 3) impedes the heat transfer to the coolant. In practical cases, these resistances are difficult to determine accurately. The contact conductance values used here were 20 to 48 kW/m^{2}K. These are high values for metallic surfaces in a vacuum, but have been obtained when the contact pressure was about 10% of the Meyer hardness of the metal (20). Although more detailed blanket design studies are required, much higher temperatures can be tolerated in the canned regions of the blanket than were found using this assumption.

There is a 20-mm layer of alumina electrical insulator between the blanket and the implosion heating coil (Fig. 3). The magnet coils must operate near room temperature, and a narrow gap between the coil and insulator would allow laminar flow of the inert gas magnet coolant. For purposes of this calculation the boundary condition was specified as helium at 300 K in laminar flow.

RESULTS

Two domains of blanket heat transfer are identified: (1) the transient start-up period when the time-averaged temperature of each blanket region approaches a constant value; (2) the steady-state regime where the temperature of each region oscillates about the time-averaged value. The transient start up begins from an initial temperature that is determined by the degree of blanket and coolant preheating and lasts for 20 to 30 5-s power cycles (Figs. 1 and 6). The most severe thermal transients are at the first wall (8).

Figure 7 gives the time dependence of temperatures in three regions of the blanket during the transient start-up period. The coolant mixed-mean temperature rise during the start up gradually increases from zero to a stable value after 20 5-s cycles. The reference case (ΔP = 51 kPa) has a low mixed-mean coolant temperature rise (maximum 57 K to minimum 11 K at end of the duty cycle), which could affect the performance of the intermediate heat exchanger. The temperature rise for the lower (ΔP = 5.1 kPa) flow is more than adequate from this viewpoint (maximum ~140 K to minimum 117 K at end of the duty cycle). Figure 8 shows the typical steady-state radial temperature profile through the blanket at the start (and end) of a duty cycle and at the end of the plasma dump when maximum first-wall temperatures are reached. Temperatures are also given for the case of the lower coolant flow (ΔP = 5.1 kPa). An indication of the axial temperature variation is given in Fig. 8 by depicting the radial temperature profile at both ends of the blanket. Examination of these and similar temperature plots leads to these observations:

- The first lead region experiences the highest temperatures in the blanket except at the end of the plasma dump when the first wall rises to about 270 K above the coolant inlet temperature.

- Temperatures generally decrease with radius across the blanket with 50 to 100 K temperature oscillations occurring within the stagnant liquid regions (no convection assumed).

- The helium coolant in the coils at the outer diameter of the blanket causes a large (~150 K) gradient in the alumina insulator at the outer radius, but no significant temperature differences occur in the bulk of the blanket.

- Temperatures in the outer portion of the blanket remain relatively constant throughout the burn at ~50 K above the reference temperature.

- The greatest axial temperature differences occur in the first wall at the end of the plasma dump.

For the corresponding temperature profiles with the lower (ΔP = 5.1 kPa) lithium flow, the same general conclusions apply except that the temperature extremes are up to 55% greater. Although maximum temperatures at the first wall are greater than with the reference (ΔP = 51 kPa) flow, the first-wall temperature change during a burn cycle shows no strong dependence on the coolant flow rate.

SUMMARY

For the duty cycle considered all blanket regions reach maximum temperatures at the end of the thermonuclear burn. These maxima are, respectively, 240 K, 160 K, 120 K, and 80 K above the coolant inlet temperature for lead, Li-6, iron, and boron-carbide. The maximum axial temperature difference in the blanket is 160 K and occurs in the first wall at the end of the plasma dump. Parametric studies that vary both ΔP and the geometry (size, position, number) of the lithium coolant channels will show that both local and average temperature variations in both space and time can be made less pronounced than those computed for the extreme cases shown in Fig. 8.

ACKNOWLEDGMENTS

The authors would like to thank S. A. W. Gerstl for providing the neutron and gamma heating distributions and R. L. Miller for the plasma energy and bremsstrahlung flux. This work was performed under the auspices of the U. S. ERDA.

REFERENCES

1. Moir, R. W., et al., Mirror Reactor Studies, Proceedings of the Sixth International Conference on Plasma Physics and Controlled Nuclear Fusion Research, Berchtesgaden, FRG, paper (I/2), October 6-13, 1976.
2. Stacey, W. M., Baker, C. C., and Roberts, M., Tokamak Experimental Power Reactor, paper (I/3-2), ibid.
3. Krakowski, R. A., et al., Pure-Fusion and Fusion-Fission Applications of High Density Linear Confinement Systems, paper (I/4), ibid.
4. Krakowski, R. W., Quinn, W. E., Ribe, F. L., and Thomas, K. W., Nucl. Eng. International, 45, February, 1977.
5. Proceedings of the Second Topical Meeting on the Technology of Controlled Nuclear Fusion, CONF-760935-P4, 2, Chapter 5, 371-538, September, 1976.
6. Misra, B., Stevens, H. C., and Maroni, V. A., Thermal Hydraulic and Power Cycle Analysis of Liquid Lithium Blanket Designs, Proceedings of the 1977 National Heat Transfer Conference, Salt Lake City, Utah, August 15-17, 1977.
7. Powell, J. R., Fillo, J. A., Twining, B. G., and Dorning, J. J. (eds.), Proceedings of the Magnetic Fusion Energy Blanket and Shielding Workshop: A Technical Assessment, USERDA Report ERDA-76/117/1, August, 1975.
8. Krakowski, R. A., Hagenson, R. L., and Cort, G. E., Nucl. Technol., 34, p. 217-241, 1977.
9. Simmons, E. L., Dudziak, D. J., and Gerstl, S. A. W., Reference Theta-Pinch Reactor (RTPR) Neutronic Design Sensitivity Analysis by Perturbation Theory, USERDA Report LA-6572-MS, April, 1976.
10. Gerstl, S. A. W., private communication. Los Alamos Scientific Laboratory, 1977.
11. ASHARE Handbook and Product Directory, American Society of Heating, Refrigeration and Air-Conditioning Engineers, Inc., New York, 1974.
12. Krakowski, R. A., Ribe, F. L., Coultas, T. A., and Hatch, A. J., An Engineering Design of a Reference Theta-Pinch Reactor (RTPR), USERDA Report LA-5336/ANL-8013, March, 1974.
13. Lawton, R. G., The AYER Heat Conduction Computer Program, USERDA Report LA-5613-MS, May 1974.
14. Gryczkowski, G. R., and Oliphant, T. A., Nucl. Fusion 16, 2,263, 1976.
15. Eckert, E. R. G., Drake, R. M., Jr., Heat and Mass Transfer, McGraw-Hill, 1959.
16. White, F. M., Viscous Fluid Flow, 1st Edition, p. 560, McGraw Hill, 1974.
17. Spalding, D. B., J. Appl. Mech. 28, 455, 1961.
18. Martinelli, R. C., Transactions ASME 69, 947 (1947).
19. Lyon, R. N., Liquid Metals Handbook, NAVEXOS P-733 (Rev), 1952.
20. Fried, E., and Costello, F. A., ARS Journal 32, 237, 1962.

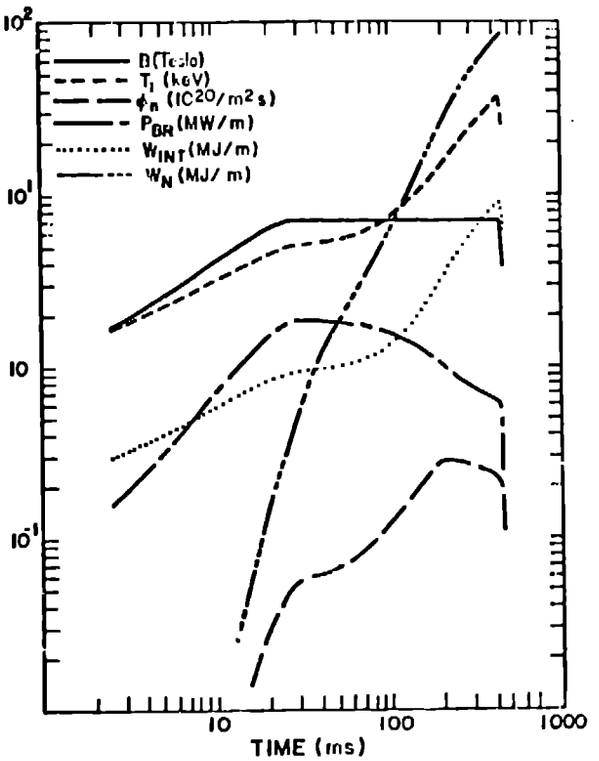

Fig. 1 RTPR Time-dependent Parameters: magnetic field, ——— ; ion temperature, - - - - ; neutron flux at first wall, — — ; bremsstrahlung power, —— - ; plasma internal energy, ... ; and neutron energy, —— ---.

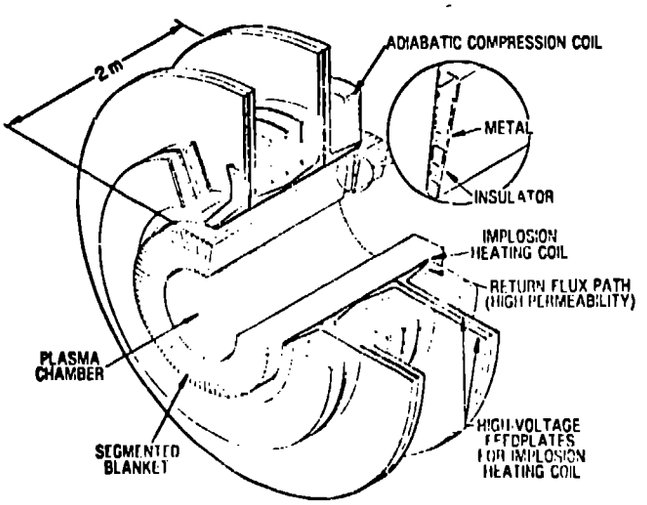

Fig. 2 Arrangement of blanket, magnetic coils, and plasma in a pulsed fusion reactor module.

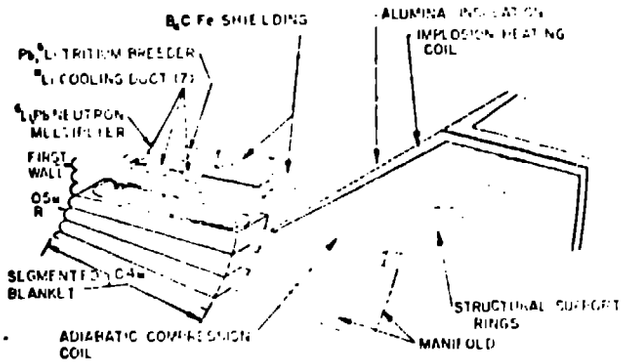

Fig. 3 Blanket structure and flow manifold.

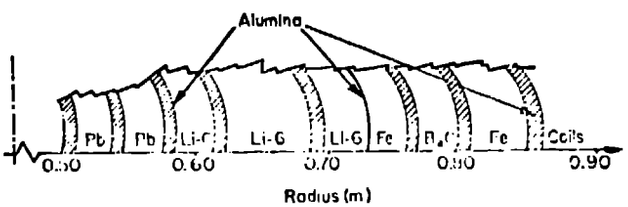

Fig. 4 Neutronic and heat-transfer model used in these calculations.

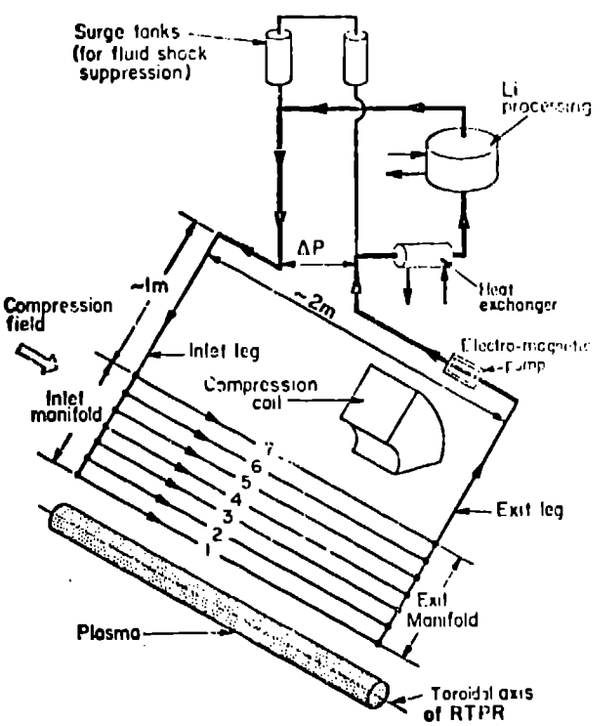

Fig. 5 Flow diagram used to describe the transient and steady-state flow conditions in a 2-m reactor module.

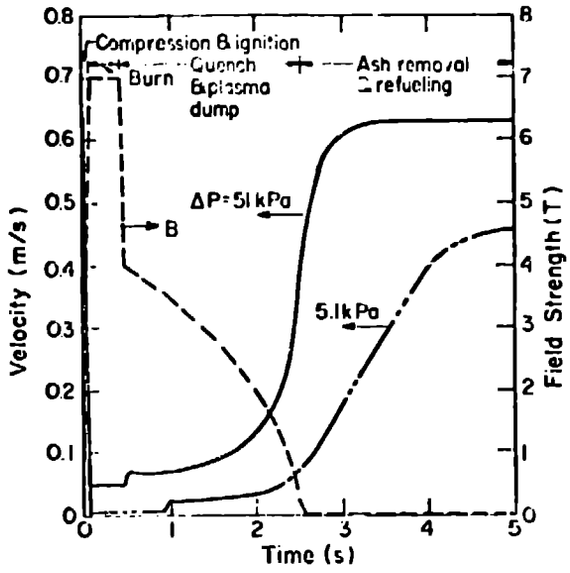

Fig. 6 Magnetic field and lithium flow velocity in inlet (and exit) leg to blanket segment.

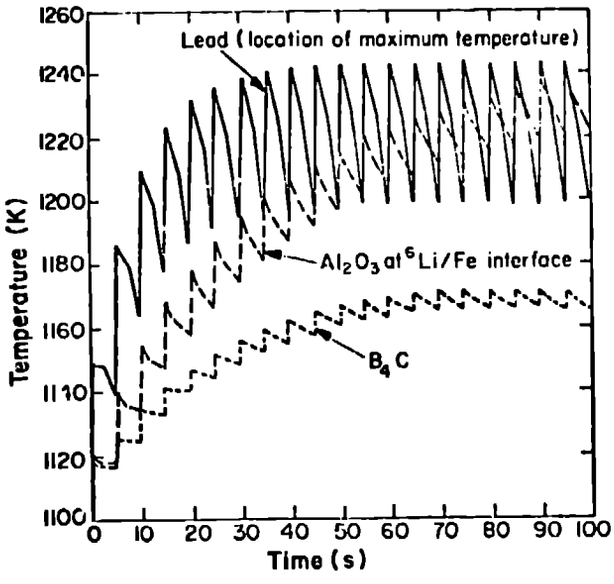

Fig. 7 Time dependence of temperatures at selected points in the blanket during start up.

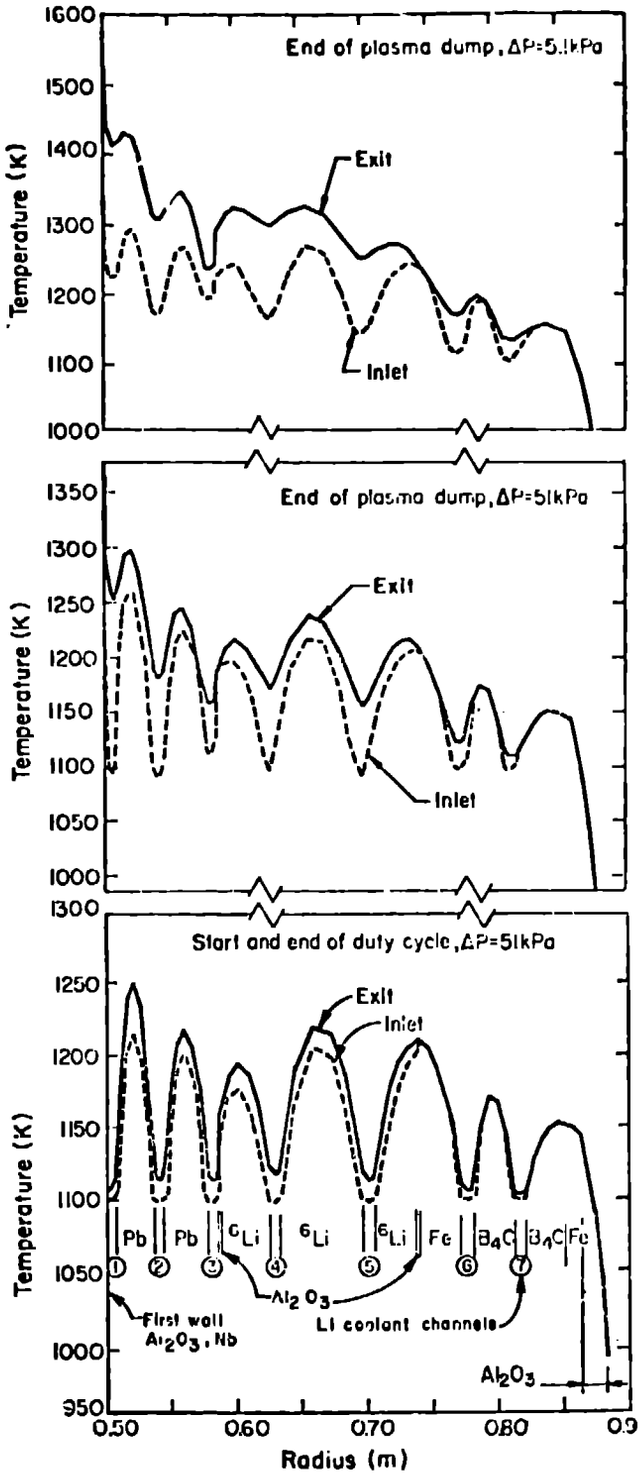

Fig. 8 Radial temperature distribution at various times during the duty cycle.